Accepted Manuscript

Discovery of novel Ponatinib analogues for reducing KDR activity as potent FGFRs inhibitors

Dr Yang Liu, Xia Peng, Xiaocong Guan, Dong Lu, Yong Xi, Shiyu Jin, Hui Chen, Limin Zeng, Jing Ai, Meiyu Geng, Youhong Hu

PII: S0223-5234(16)30865-0

DOI: 10.1016/j.ejmech.2016.10.003

Reference: EJMECH 8968

To appear in: *European Journal of Medicinal Chemistry*

Received Date: 1 August 2016

Revised Date: 1 October 2016

Accepted Date: 1 October 2016

Please cite this article as: D.Y. Liu, X. Peng, X. Guan, D. Lu, Y. Xi, S. Jin, H. Chen, L. Zeng, J. Ai, M. Geng, Y. Hu, Discovery of novel Ponatinib analogues for reducing KDR activity as potent FGFRs inhibitors, *European Journal of Medicinal Chemistry* (2016), doi: 10.1016/j.ejmech.2016.10.003.

Title:

Discovery of Novel Ponatinib Analogues for Reducing KDR Activity as Potent FGFRs Inhibitors

Graphical abstract

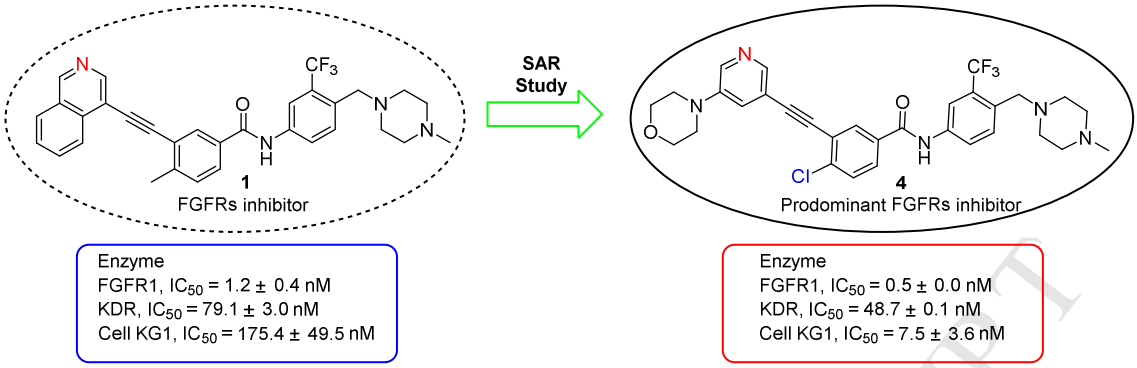

Enzyme
FGFR1, IC_{50} = 1.2 ± 0.4 nM
KDR, IC_{50} = 79.1 ± 3.0 nM
Cell KG1, IC_{50} = 175.4 ± 49.5 nM

Enzyme
FGFR1, IC_{50} = 0.5 ± 0.0 nM
KDR, IC_{50} = 48.7 ± 0.1 nM
Cell KG1, IC_{50} = 7.5 ± 3.6 nM

A series of novel Ponatinib analogues were synthesized. Observations made in a structure and activity relationship (SAR) investigation led to compound **4** as a predominant FGFR inhibitor.

Highlights

- Novel Ponatinib analogues as selective FGFRs inhibitors were synthesized.
- The SAR of these novel Ponatinib analogues were investigated.
- The target selectivity for FGFR1 over KDR was improved by structural optimization.
- Lead compound with both high potent enzymatic and cellular activity was achieved.
- The evaluation of the lead compound **4** in *vivo* was reported.

Title:

Discovery of Novel Ponatinib Analogues for Reducing KDR Activity as Potent FGFRs Inhibitors

Dr. Yang Liu,[†, §] Xia Peng,[‡, §] Xiaocong Guan,[†, §] Dong Lu,[†] Yong Xi,[‡] Shiyu Jin,[†] Hui Chen,[‡] Limin Zeng,[†] Jing Ai,[*, ‡] Meiyu Geng,[*, ‡] and Youhong Hu[*, †]

[†]State Key Laboratory of Drug Research, Shanghai Institute of Materia Medica, Chinese Academy of Sciences, 555 ZuChongZhi Road, Shanghai, 201203, China.

[‡]Division of Anti-Tumor Pharmacology, State Key Laboratory of Drug Research, Shanghai Institute of Materia Medica, Chinese Academy of Sciences, 555 ZuChongZhi Road, Shanghai, 201203, China

[*]Corresponding author: E-mail: yhhu@simm.ac.cn, mygeng@simm.ac.cn, jai@simm.ac.cn.

[§]Y. L., X. P. and X. G. contributed equally to this work

Abstract:

FGF receptors (FGFRs) are tyrosine kinases that are overexpressed in diverse tumors by genetic alterations such as gene amplifications, somatic mutations and translocations. Owing to this characteristic, FGFRs are attractive targets for cancer treatment. It has been demonstrated that most multi-targeted, ATP competitive tyrosine kinase inhibitors are active against FGFRs as well as other kinases. The design of new and more selective inhibitors of FGFRs, which might be reduced off-target and side effects, is a difficult yet significant challenge. The results of the current investigation, show that novel Ponatinib analogues are highly active as FGFR inhibitors and that they possess reduced kinase insert domain receptor (KDR) activities. Observations made in a structure and activity relationship (SAR) investigation led to the development of a promising, orally available lead compound **4**, which displays a 50-100 fold in *vitro* selectivity for inhibition of FGFR1-3 over KDR. In addition, biological evaluation of compound **4** showed that it displays significant antitumor activities in FGFR1-amplificated H1581 and FGFR2-amplificated SNU-16 xenograft models.

Key words:

FGFR / KDR/ inhibitor/ anticancer/ Ponatinib

1. Introduction

The fibroblast growth factor/fibroblast growth factor receptor (FGF/FGFR) signaling pathway plays a fundamental role in many physiological processes, including embryogenesis, adult tissue homeostasis and wound healing [1-3]. Substantial evidence has been accumulated that the aberrant FGFR signaling is activated in diverse tumor types by genetic alterations including genetic amplifications, somatic mutations and translocations [4-6]. Moreover, the results of studies using preclinical models and patient biomarker validation have demonstrated the oncogenic potential of these aberrations in driving tumor growth, promoting tumor metastasis as well as conferring

resistance to anticancer therapies [7-11]. Consequently, the targeted inhibition of FGFRs is an attractive modality for cancer treatment. However, most multi-targeted, ATP competitive tyrosine kinase inhibitors are active against FGFRs as well as other kinases. The lack of kinase selectivity of these inhibitors has the potential of causing significant side effects [12-14]. For example, their activity against VEGF receptor 2 (VEGFR2, KDR) is the likely source of grade 3/4 hypertension induction and dose-limiting toxicity of these inhibitors [15,16]. The discovery of substances that selectively inhibit kinases is a difficult yet significant challenge [17-22].

Ponatinib (AP24534, Figure 1) is a multi-targeted tyrosine kinase inhibitor that exhibits potent inhibitory activity against many tyrosine kinases including Abl, Src, PDGFRα, FGFR1 and KDR with respective IC_{50} values of 0.37 nM, 2.5 nM, 2.6 nM, 1.2 nM and 3.7 nM [23,24]. As can be seen by viewing the information in Figure 1, changes in the nature of the heterocyclic ring system attached to the Ponatinib core structure alter the specificities of binding to various kinases. This feature has been used advantageously to uncover selective Bcr-Abl inhibitors, which do not suffer from drug resistance [25-29], as well as selective DDR1 [30] and Src inhibitors [31] (Figure 1). In our group, compound **1** as an analogue of ponatinib was identified for a potent FGFR1 inhibitor with an IC_{50} value of 1.2 nM and a weaker activity against KDR with an IC_{50} of 79.1 nM at the enzymatic level. While the activity of **1** against FGFR1 translocated KG1 cells is only modest (IC_{50} = 175.5 nM). A following structure activity relationship (SAR) investigation based on compound **1** led to the development of a promising, orally available substance **4** which displays a 50-100 fold in vitro selectivity for inhibition of FGFR1-3 over VEGFR1-2. In addition, biological evaluation of this substance **4** showed that it displays significant antitumor activities in FGFR1-amplificated H1581 and FGFR2-amplificated SNU-16 xenograft models.

Figure 1

2. Results and Discussion

2.1 Chemistry

The designed compounds for SAR investigation focused on the modification of various six-membered aryl ring for A while retaining the isoquinoline group and changing the B ring component while retaining the methyl-substituted phenyl ring (Scheme 1). The general pathway employed to prepare these targets is depicted in Scheme 1. The routes begin with transformation of the appropriate halogen-substituted aryl acid **5** to the corresponding acyl chloride, which is then reacted with the piperazine containing aniline derivative. This process forms amide **6**, which is then coupled with the appropriate TMS-substituted alkyne to generate the target compound.

Scheme 1

2.2 SAR study and lead generation

The initial FGFR1 enzyme inhibition of the compounds that focused on the modification of various six-membered aryl ring A was tested, and then the potent inhibitors were further investigated against the FGFR1-translocated KG1 cell and KDR profiles (Table 1). As can be seen by viewing the data listed in Table 1, removal of the methyl group on the phenyl A-ring or replacement of it by a fluorine group (**2a** and **2b**, respectively) lead to an improved cellular activity but a diminished FGFR1/KDR selectivity. In contrast, replacing the methyl group by a chlorine substituent (**2c**) dramatically enhances the cellular activity while maintaining enzyme selectivity. In addition, introduction of electron donating or withdrawing group (**2d** and **2e**) and a

bulky group (**2f**) in place of the methyl group on the A-ring phenyl moiety cause a decrease in FGFR1 inhibitory activity. Moreover, replacement of the phenyl ring by variously positioned pyridine groups (**2g-2k**) do not bring about improvement of cellular activity or selectivity. These observations indicate that the substituents on the phenyl A-ring have a significant effect on enzymatic activity and selectivity of the Ponatinib analogues.

Table 1

Meanwhile, the enzyme and cell level inhibitory properties of Ponatinib analogues containing the methyl-substituted phenyl A-ring and diverse N-heterocycles as the B-ring unit (Table 2) were also explored. The results show that **3a-3b** with N-heteroindole display an observable selectivity for FGFR1 over KDR. After opened the indole ring to the different N-substituted pyridines, **3c-3g** also exhibit the promised selectivity. The methoxyl substituted compound **3h** decrease the activity of FGFR1 slightly. Significantly, **3b** and **3f** have excellent selectivity and inhibitory activities for KG1 cells.

The results of this effort show that **2c**, which contains a chloro-phenyl A-ring, and **3f**, which contains a morpholine substituted pyridine group as the B-ring, have ideal properties. This finding led to the design and synthesis of derivative **4** (see Table 2), which exhibits potent inhibitory activity against FGFR1 (IC_{50} = 0.5 nM), weak KDR inhibitory activity (IC_{50} = 48.7 nM) and a potent KG1 cellular activity ((IC_{50} = 7.4 nM) as expected.

Table 2

The kinase inhibition profiles and selected anti-proliferation activities in related cell lines of the newly designed inhibitor **4** were furtherly evaluated and contrasted with Ponatinib (Table 3). The results show that **4** has a significantly higher potency against FGFRs and displays a greater inhibitory selectivity for KDR and VEGFR1 than does Ponatinib. Paralleling these enzyme level activities, **4** exhibits anti-proliferation properties against FGFRs and KDR translocated cell lines. Interestingly, **4** inhibits RET and the RET-V804M gatekeeper mutant kinase and its driven cell growth to the same degrees that Ponatinib does [32]. In addition, the fact that **4** does not inhibit EGFR, its use as an anticancer drug could be associated with less adverse side effects. It is likely that **4** will have inhibitory activities against FGFR1-3 and reduced inhibitory activities against Src and ABL.

Table 3

The cellular kinase-targeting activity of **4** in representative FGFR1 translocated KG1 cells and FGFR2 amplified SUN16 cells was evaluated. The results show that **4** inhibits FGFR phosphorylation as well as the phosphorylation of key downstream Erk, and PLCγ proteins in a dose-dependent manner (Figure 2A and B). These findings demonstrate that **4** could be used to block the FGFR signaling pathway.

Figure 2

A preliminary study was carried out to assess the pharmacokinetic properties of **4** in mice. For this purpose, the plasma concentrations of **4**, following oral administration at a dose of 10 mg/kg, were determined (Figure 3). The results reveal that compound **4** can be absorbed and reach a high plasma concentration ($AUC_{0\text{-}24h}$ of 11.38 ug*h/mL). This property stimulated a study of the in *vivo* effects of **4** on the two representative tumor xenograft models including a FGFR1-amplificated H1581 human lung cancer model and a FGFR2-amplificated SNU-16 human gastric carcinoma

model. As shown in Figure 4, when administered orally at a dosing regimen of 20 mg/kg once daily, **4** displays significant antitumor activity in both tumor xenografts.

Figure 3

Figure 4

3. Conclusions

As described above, the SAR study based on compound **1** led to the identification of compound **4** as an ideal inhibitor. An enzyme level investigation showed that **4** is a more potent and selective FGFRs tyrosine kinase inhibitor than is Ponatinib. In addition, the use of **4** as a drug could be associated with a lower level of adverse side effects caused by VEGFR and EGFR inhibition. Finally, the results of further studies show that **4** has favorable pharmacokinetic properties in mice and better antitumor activity than does Ponatinib in a FGFR2-driven SNU-16 xenograft model. The combined observations indicate that **4** is an excellent starting point for optimization studies targeted at the development of clinical candidates for treatment of patients with FGFRs driven cancer.

4. Experimental Section

4.1 General Information

Unless otherwise noted, all reagents and solvents employed were purchased commercially and used as received. All reactions involving air- or moisture-sensitive reagents were performed under a N2 atmosphere. All reactions were conducted in microwave vials or flasks containing Teflon-coated magnetic stirrer. Microwave irradiation experiments were performed in a CEM-Discover® LabMate mono-mode microwave apparatus equipped with an IntelliVentTM pressure control system and a vertically-focused IR temperature sensor. Reactions were monitored by the thin layer chromatography (TLC) on precoated TLC glass plates (silica gel GF254, 0.2±0.03mm thickness) or by Agilent 1200 series LC-MS system (100mm x 3mm 3.5μm column + column; 5μL injection; 3-98% MeOH/H2O + 0.1% HCOOH gradient over 6 min; 0.7 mL/min flow; ESI; positive ion mode; UV detection at 254 nM). TLC glass plates were developed in a covered chamber and were visualized with ultraviolet light using a 254 nm fluorescent indicator. Low-resolution mass spectral (MS) data were gathered on the LC-MS system. Column chromatography was carried out on silica gel (200-300 mesh). All ^{1}H NMR and ^{13}C NMR spectra were measured in $CDCl_3$, CD_3OD or DMSO-d_6 with TMS as the internal standard on Varian Mercury NMR spectrometers. Chemical shifts were expressed in parts per million (ppm, δ units) and coupling constants were given in Hz. Data for NMR spectra were reported as follows: chemical shift (δ ppm), multiplicity (s = singlet, brs = broad singlet, d = doublet, t = triplet, q = quartet, dd = doublet of doublets, m = multiplet), coupling constant (Hz), integration.

4.2 Procedure for Preparation of Novel Ponatinib Analogues

*4.2.1. The Preparation of 3-(isoquinolin-4-ylethynyl)-4-methyl-N-(4-((4-methylpiperazin-1-yl) methyl)-3-(trifluoromethyl) phenyl) benzamide (**1**).*

Step 1: To a solution of 3-iodo-4-methylbenzoic acid **5-1** (262 mg, 1.0 mmol) in dry DCM (10 mL) at 0 ^{o}C was added oxalyl chloride (0.13 ml, 1.5 mmol) and 3 drops of dry DMF. The resulting reaction mixture was stirred at room temperature for 3h, and then the solvent was removed under reduced pressure. The crude product was used directly for the next step without further

purification. Step 2: To a solution of 3-iodo-4-methylbenzoyl chloride obtained above in dry DCM (10 mL) at 0 ^{o}C was added Et_3N (0.28 ml, 2.0 mmol) and 4-((4-methylpiperazin-1-yl) methyl)-3-(trifluoromethyl) aniline (328 mg, 1.2 mmol). The mixture was stirred at room temperature for 5h, and then the solvent was removed under reduced pressure. The residue was purified by using column chromatography to afford the corresponding product **6-1** (439 mg, 2 steps yield: 85%). Step 3: To a solution of **6-1** (260 mg, 0.5 mmol) in dry MeCN (2 mL) was added $Pd(PPh_3)_4$ (30 mg, 0.025 mmol), CuI (10 mg, 0.05 mmol), Et_3N (0.28 ml, 2.0 mmol), CsF (152 mg, 1.0 mmol) and 4-((trimethylsilyl) ethynyl) isoquinoline **7-1** (225 mg, 1.0 mmol) at room temperature under nitrogen atmosphere. After stirring for 5 min, the mixture was irradiated for 15 min at 90 °C (monitored by TLC). The mixture was extracted with ethyl acetate (10 mL×3). The combined organic layers were washed with brine (10 mL), dried over anhydrous Na_2SO_4, filtered and concentrated to give the crude product, which was further purified by column chromatography to afford compound **1** as a light yellow solid (176 mg, yield 65%): mp 128~130 ℃. ^{1}H NMR (400 MHz, $CDCl_3$) δ 9.51 (s, 1H), 9.14 (s, 1H), 8.68 (s, 1H), 8.23 (d, *J* = 5.0 Hz, 2H), 8.10 (s, 1H), 8.02 (d, *J* = 8.3 Hz, 1H), 7.93 (t, *J* = 9.1 Hz, 2H), 7.74 (t, *J* = 7.5 Hz, 1H), 7.62 (t, *J* = 7.5 Hz, 1H), 7.53 (d, *J* = 8.6 Hz, 1H), 7.31 (d, *J* = 8.2 Hz, 1H), 3.62 (s, 2H), 3.00 (s, 4H), 2.74 (s, 4H), 2.65 (s, 3H), 2.57 (s, 3H).^{13}C NMR (151 MHz, $CDCl_3$) δ 165.59, 152.01, 146.16, 144.30, 137.96, 135.32, 131.99, 131.48, 131.39, 131.27, 129.97, 129.18 (q, *J* = 30.5 Hz), 128.10, 128.05, 127.99, 127.73, 124.93, 124.04 (q, *J* = 273.31 Hz), 123.81, 122.96, 118.48 (d, *J* = 5.8 Hz), 115.94, 94.68, 89.18, 57.38, 54.07, 49.97, 43.85, 21.05.^{19}F NMR (471 MHz, $CDCl_3$) δ -59.08. HRMS $[M]^+$ Calculated for $C_{32}H_{29}F_3N_4O$ 542.2293, found 542.2295.

*4.2.2. The Preparation of 3-(isoquinolin-4-ylethynyl)-N-(4-((4-methylpiperazin-1-yl) methyl)-3-(trifluoromethyl) phenyl) benzamide (**2a**).*

The procedures applied to the synthesis of **1** were used with 3-iodobenzoic acid **5-2a** (62 mg, 0.25 mmol), 4-((4-methylpiperazin-1-yl) methyl)-3-(trifluoromethyl) aniline, (82 mg, 0.30 mmol) and 4-((trimethylsilyl) ethynyl) isoquinoline **7-1** (112 mg, 0.50 mmol) to obtain **2a** as a white solid (87 mg, yield: 66%): mp 118~120 ℃. ^{1}H NMR (400 MHz, $CDCl_3$) δ 9.25 (s, 1H), 9.18 (s, 1H), 8.73 (s, 1H), 8.29 (s, 1H), 8.26 (s, 1H), 8.07 (s, 1H), 8.02 (d, *J* = 8.1 Hz, 2H), 7.98 (d, *J* = 8.2 Hz, 1H), 7.82 – 7.72 (m, 2H), 7.66 (t, *J* = 7.5 Hz, 1H), 7.59 (d, *J* = 8.4 Hz, 1H), 7.51 (t, *J* = 7.8 Hz, 1H), 3.66 (s, 2H), 2.95 (s, 4H), 2.75 (s, 4H), 2.62 (s, 3H).^{13}C NMR (126 MHz, $CDCl_3$) δ 164.95, 151.71, 145.83, 137.17, 134.97, 134.39, 134.27, 131.38, 131.02, 130.98, 130.24, 128.87 (q, *J* = 30.24 Hz), 128.52, 127.65, 127.53, 127.43, 127.25, 124.49, 123.52 (q, *J* = 274.4 Hz), 123.25, 122.87, 117.96 (d, *J* = 5.8 Hz), 115.16, 95.14, 85.08, 56.99, 53.72, 49.79, 43.61.^{19}F NMR (471 MHz, $CDCl_3$) δ -59.18. HRMS $[M]^+$ Calculated for $C_{31}H_{27}F_3N_4O$ 528.2137, found 528.2132.

*4.2.3. The Preparation of 4-fluoro-3-(isoquinolin-4-ylethynyl)-N-(4-((4-methylpiperazin-1-yl) methyl)-3-(trifluoromethyl) phenyl) benzamide (**2b**).*

The procedures applied to the synthesis of **1** were used with 4-fluoro-3-iodobenzoic acid **5-2b** (66 mg, 0.25 mmol), 4-((4-methylpiperazin-1-yl) methyl)-3-(trifluoromethyl) aniline **8** (82 mg, 0.30 mmol) and 4-((trimethylsilyl)ethynyl) isoquinoline **7-1** (112 mg, 0.50 mmol) to obtain **2b** as a white solid (83 mg, yield: 61%): mp 118~120 ℃. ^{1}H NMR (400 MHz, $CDCl_3$) δ 9.25 (s, 1H), 9.20 (s, 1H), 8.76 (s, 1H), 8.30 (d, *J* = 8.0 Hz, 2H), 8.02 (dd, *J* = 18.5, 10.6 Hz, 4H), 7.81 (t, *J* = 7.6 Hz, 1H), 7.71 – 7.59 (m, 2H), 7.25 (t, *J* = 8.6 Hz, 1H), 3.66 (s, 2H), 2.88 (s, 3H), 2.72 (s, 4H), 2.58 (s, 3H).^{13}C NMR (126 MHz, $CDCl_3$) δ 164.08 (d, *J* =259.56 Hz), 163.98, 152.03, 145.87,

137.00, 134.94, 132.43, 131.73, 131.19, 131.00, 130.25 (d, *J* = 3.2 Hz), 129.84 (d, *J* = 8.9 Hz), 128.85 (q, *J* = 30.7 Hz), 127.75, 127.53, 127.24, 124.49, 123.53 (q, *J* = 274.1 Hz), 123.25, 117.90 (d, *J* = 5.9 Hz), 115.66 (d, *J* = 21.6 Hz), 114.91, 111.48 (d, *J* = 16.7 Hz), 90.14, 88.56, 57.05, 53.89, 50.24, 43.92. ^{19}F NMR (471 MHz, $CDCl_3$) δ -59.29, -103.84. HRMS $[M]^+$ Calculated for $C_{31}H_{26}F_4N_4O$ 546.2043, found 546.2041.

*4.2.4. The Preparation of 4-chloro-3-(isoquinolin-4-ylethynyl)-N-(4-((4-methylpiperazin-1-yl) methyl)-3-(trifluoromethyl) phenyl) benzamide (**2c**).*

The procedures applied to the synthesis of **1** were used with 4-chloro-3-iodobenzoic acid **5-2c** (70 mg, 0.25 mmol), 4-((4-methylpiperazin-1-yl) methyl)-3-(trifluoromethyl) aniline (82 mg, 0.30 mmol) and 4-((trimethylsilyl)ethynyl) isoquinoline **7-1** (112 mg, 0.50 mmol) to obtain **2c** as a white solid (97 mg, yield: 69%): mp 132~134 ℃. ^{1}H NMR (400 MHz, $CDCl_3$) δ 9.41 (s, 1H), 9.19 (s, 1H), 8.76 (s, 1H), 8.37 (d, *J* = 8.4 Hz, 1H), 8.31 (d, *J* = 2.0 Hz, 1H), 8.08 (s, 1H), 8.04 (d, *J* = 8.5 Hz, 1H), 8.01 – 7.95 (m, 2H), 7.80 (t, *J* = 7.6 Hz, 1H), 7.67 (t, *J* = 7.5 Hz, 1H), 7.60 (d, *J* = 8.4 Hz, 1H), 7.56 (d, *J* = 8.4 Hz, 1H), 3.67 (s, 2H), 2.95 (s, 4H), 2.75 (s, 4H), 2.63 (s, 3H).^{13}C NMR (126 MHz, $CDCl_3$) δ 164.09, 152.01, 146.06, 139.09, 137.11, 134.98, 132.49, 131.87, 131.46, 131.16, 131.01, 129.29, 128.86 (q, *J* = 30.24 Hz), 128.42, 127.72, 127.49, 127.25, 124.62,123.73 (q, *J* = 275.94 Hz), 123.27, 122.68, 117.98 (d, *J* = 5.9 Hz), 114.93, 92.03, 90.23, 57.00, 53.74, 49.82, 43.63.^{19}F NMR (471 MHz, $CDCl_3$) δ -59.16. HRMS $[M]^+$ Calculated for $C_{31}H_{26}ClF_3N_4O$ 562.1747, found 562.1751.

*4.2.5. The Preparation of 3-(isoquinolin-4-ylethynyl)-4-methoxy-N-(4-((4-methylpiperazin-1-yl) methyl)-3-(trifluoromethyl) phenyl) benzamide (**2d**).*

The procedures applied to the synthesis of **1** were used with 3-iodo-4-methoxybenzoic acid **5-2d** (70 mg, 0.25 mmol), 4-((4-methylpiperazin-1-yl) methyl)-3-(trifluoromethyl) aniline (82 mg, 0.30 mmol) and 4-((trimethylsilyl)ethynyl) isoquinoline **7-1** (112 mg, 0.50 mmol) to obtain **2d** as an off-white solid (70 mg, yield: 50%): mp 112~114 ℃. ^{1}H NMR (400 MHz, $CDCl_3$) δ 9.16 (d, *J* = 12.6 Hz, 1H), 9.13 (s, 1H), 8.72 (s, 1H), 8.30 (d, *J* = 8.4 Hz, 1H), 8.15 (d, *J* = 1.9 Hz, 1H), 8.01 – 7.91 (m, 4H), 7.71 (dd, *J* = 14.0, 7.5 Hz, 2H), 7.61 (t, *J* = 7.5 Hz, 1H), 6.95 (d, *J* = 8.8 Hz, 1H), 3.98 (s, 3H), 3.62 (s, 2H), 2.55 (s, 8H), 2.34 (s, 3H).^{13}C NMR (126 MHz, $CDCl_3$) δ 165.12, 162.75, 151.91, 145.93, 137.27, 135.57, 133.08, 132.29, 131.30, 130.33, 129.11 (q, *J* = 30.5 Hz), 128.00, 127.86, 127.75, 126.74, 125.18, 124.11 (q, *J* = 272.16 Hz), 123.56, 123.02, 117.95 (d, *J* = 5.9 Hz), 116.12, 112.18, 110.66, 92.36, 89.33, 57.75, 56.19, 55.01, 52.53, 45.64.^{19}F NMR (471 MHz, $CDCl_3$) δ -59.30. HRMS $[M]^+$ Calculated for $C_{32}H_{29}F_3N_4O_2$ 558.2243, found 558.2241.

*4.2.6. The Preparation of 3-(isoquinolin-4-ylethynyl)-N-(4-((4-methylpiperazin-1-yl) methyl)-3-(trifluoromethyl) phenyl)-4-(trifluoromethyl) benzamide (**2e**).*

The procedures applied to the synthesis of **1** were used with 3-iodo-4-(trifluoromethyl) benzoic acid **5-2e** (79 mg, 0.25 mmol), 4-((4-methylpiperazin-1-yl) methyl)-3-(trifluoromethyl) aniline (82 mg, 0.30 mmol) and 4-((trimethylsilyl)ethynyl) isoquinoline **7-1** (112 mg, 0.50 mmol) to obtain **2e** as a white solid (67 mg, yield: 45%): mp 106~108 ℃. ^{1}H NMR (400 MHz, $CDCl_3$) δ 9.63 (s, 1H), 9.15 (s, 1H), 8.73 (s, 1H), 8.34 (s, 1H), 8.20 (d, *J* = 8.3 Hz, 1H), 8.04 (dd, *J* = 13.3, 6.1 Hz, 3H), 7.95 (d, *J* = 8.2 Hz, 1H), 7.76 (dd, *J* = 14.6, 8.0 Hz, 2H), 7.69 (d, *J* = 8.4 Hz, 1H), 7.64 (t, *J* = 7.5 Hz, 1H), 3.64 (s, 2H), 2.65 (d, *J* = 22.1 Hz, 8H), 2.44 (s, 3H).^{13}C NMR (126 MHz, $CDCl_3$) δ 164.33, 152.64, 146.68, 137.71, 137.05, 135.45, 133.81 (q, *J* = 30.9 Hz), 133.24, 132.97, 131.72,

131.42, 129.28 (q, *J* = 30.5 Hz), 128.27, 127.94, 127.72, 126.56 (d, *J* = 4.8 Hz), 124.83, 124.01 (q, *J* = 274.2 Hz), 123.77, 123.11 (q, *J* = 273.8 Hz), 118.29 (d, *J* = 5.9 Hz), 115.30, 91.50, 91.23, 57.63, 54.76, 51.78, 45.11.^{19}F NMR (471 MHz, $CDCl_3$) δ -59.33, -62.33. HRMS $[M]^+$ Calculated for $C_{32}H_{26}F_6N_4O$ 596.2011, found 596.2016.

*4.2.7. The Preparation of 4-isopropyl-3-(isoquinolin-4-ylethynyl)-N-(4-((4-methylpiperazin-1-yl) methyl)-3-(trifluoromethyl) phenyl) benzamide (**2f**).*

The procedures applied to the synthesis of **1** were used with 3-iodo-4-isopropylbenzoic acid **5-2f** (73 mg, 0.25 mmol), 4-((4-methylpiperazin-1-yl) methyl)-3-(trifluoromethyl) aniline (82 mg, 0.30 mmol) and 4-((trimethylsilyl)ethynyl) isoquinoline **7-1** (112 mg, 0.50 mmol) to obtain **2f** as an off-white solid (61 mg, yield: 43%): mp 112~114 ℃. ^{1}H NMR (400 MHz, $CDCl_3$) δ 9.20 (s, 1H), 9.00 (s, 1H), 8.75 (s, 1H), 8.26 (d, *J* = 8.4 Hz, 1H), 8.23 (d, *J* = 1.4 Hz, 1H), 8.07 – 7.95 (m, 4H), 7.79 (t, *J* = 7.6 Hz, 1H), 7.68 (d, *J* = 7.5 Hz, 1H), 7.63 (d, *J* = 8.8 Hz, 1H), 7.46 (d, *J* = 8.2 Hz, 1H), 3.74 – 3.60 (m, 3H), 2.85 (s, 4H), 2.71 (s, 4H), 2.55 (s, 3H), 1.39 (s, 3H), 1.37 (s, 3H).^{13}C NMR (126 MHz, $CDCl_3$) δ 166.02, 155.36, 152.83, 147.06, 138.26, 136.15, 132.86, 132.69, 132.22, 132.13, 130.09 (q, *J* = 30.6 Hz), 128.94, 128.79, 128.74, 128.52, 126.42, 125.63, 124.74 (q, *J* = 274.2 Hz), 124.27, 122.90, 118.92 (d, *J* = 5.8 Hz), 116.66, 95.09, 89.83, 58.29, 55.10, 51.56, 45.18, 32.76, 30.40, 23.65.^{19}F NMR (471 MHz, $CDCl_3$) δ -59.25. HRMS $[M]^+$ Calculated for $C_{34}H_{33}F_3N_4O$ 570.2606, found 570.2608.

*4.2.8. The Preparation of 4-(isoquinolin-4-ylethynyl)-N-(4-((4-methylpiperazin-1-yl) methyl)-3-(trifluoromethyl) phenyl) picolinamide (**2g**).*

The procedures applied to the synthesis of **1** were used with 4-bromopicolinic acid **5-2g** (51 mg, 0.25 mmol), 4-((4-methylpiperazin-1-yl) methyl)-3-(trifluoromethyl) aniline (82 mg, 0.30 mmol) and 4-((trimethylsilyl)ethynyl) isoquinoline **7-1** (112 mg, 0.50 mmol) to obtain **2g** as a brown solid (47 mg, yield: 36%): mp 115~117 ℃. ^{1}H NMR (400 MHz, $CDCl_3$) δ 10.11 (s, 1H), 9.27 (s, 1H), 8.82 (s, 1H), 8.67 (d, *J* = 5.0 Hz, 1H), 8.48 (s, 1H), 8.30 (d, *J* = 8.4 Hz, 1H), 8.09 – 7.99 (m, 3H), 7.87 (t, *J* = 7.6 Hz, 1H), 7.71 (dd, *J* = 15.5, 6.2 Hz, 3H), 3.71 (s, 2H), 2.85 (s, 4H), 2.75 (s, 4H), 2.57 (s, 3H).^{13}C NMR (126 MHz, $CDCl_3$) δ 161.17, 152.75, 149.08, 147.78, 146.75, 136.25, 134.91, 132.58, 131.96, 131.22 (d, *J* = 8.2 Hz), 129.12 (q, *J* = 30.7 Hz), 127.82, 127.74, 127.69, 127.24, 124.24, 124.07, 123.52 (q, *J* = 274.3 Hz), 122.15, 116.94 (d, *J* = 6.0 Hz), 113.98, 92.56, 90.25, 57.16, 54.00, 50.61, 44.18.^{19}F NMR (471 MHz, $CDCl_3$) δ -59.12. HRMS $[M]^+$ Calculated for $C_{30}H_{26}F_3N_5O$ 529.2089, found 529.2096.

*4.2.9. The Preparation of 6-(isoquinolin-4-ylethynyl)-N-(4-((4-methylpiperazin-1-yl) methyl)-3-(trifluoromethyl) phenyl) picolinamide (**2h**).*

The procedures applied to the synthesis of **1** were used with 6-bromopicolinic acid **5-2h** (51 mg, 0.25 mmol), 4-((4-methylpiperazin-1-yl) methyl)-3-(trifluoromethyl) aniline (82 mg, 0.30 mmol) and 4-((trimethylsilyl)ethynyl) isoquinoline **7-1** (112 mg, 0.50 mmol) to obtain **2h** as a light brown solid (52 mg, yield: 39%): mp 118~120 ℃. ^{1}H NMR (400 MHz, $CDCl_3$) δ 10.11 (s, 1H), 9.32 (s, 1H), 8.93 (s, 1H), 8.41 (d, *J* = 8.4 Hz, 1H), 8.34 (d, *J* = 7.8 Hz, 1H), 8.13 – 8.00 (m, 4H), 7.91 (d, *J* = 7.8 Hz, 1H), 7.88 (d, *J* = 7.6 Hz, 1H), 7.76 (t, *J* = 7.6 Hz, 1H), 7.68 (d, *J* = 8.5 Hz, 1H), 3.77 (s, 2H), 3.03 (s, 4H), 2.86 (s, 4H), 2.70 (s, 3H).^{13}C NMR (151 MHz, $CDCl_3$) δ 161.60, 153.18, 149.80, 147.40, 141.64, 138.27, 136.92, 135.57, 130.45, 127.99(q, *J* = 30.6 Hz), 128.31, 128.25, 127.79, 124.88, 123.77 (q, *J* = 273.32 Hz), 122.87, 122.11, 117.84 (d, *J* = 5.7 Hz), 114.51,

94.56, 85.73, 57.64, 54.22, 50.26, 44.14.^{19}F NMR (471 MHz, $CDCl_3$) δ -59.35. HRMS $[M]^+$ Calculated for $C_{30}H_{26}F_3N_5O$ 529.2089, found 529.2091.

*4.2.10. The Preparation of 5-(isoquinolin-4-ylethynyl)-N-(4-((4-methylpiperazin-1-yl) methyl)-3-(trifluoromethyl) phenyl) nicotinamide (**2i**).*

The procedures applied to the synthesis of **1** were used with 5-bromonicotinic acid **5-2i** (51 mg, 0.25 mmol), 4-((4-methylpiperazin-1-yl) methyl)-3-(trifluoromethyl) aniline (82 mg, 0.30 mmol) and 4-((trimethylsilyl)ethynyl) isoquinoline **7-1** (112 mg, 0.50 mmol) to obtain **2i** as a brown solid (54 mg, yield: 41%): mp 106~108 ℃. ^{1}H NMR (400 MHz, $CDCl_3$) δ 9.75 (s, 1H), 9.23 (d, *J* = 1.9 Hz, 1H), 9.20 (s, 1H), 8.93 (d, *J* = 1.7 Hz, 1H), 8.74 (s, 1H), 8.56 (d, *J* = 1.9 Hz, 1H), 8.26 (d, *J* = 8.3 Hz, 1H), 8.10 (s, 1H), 8.05 (d, *J* = 8.3 Hz, 1H), 8.00 (d, *J* = 8.2 Hz, 1H), 7.82 (t, *J* = 7.6 Hz, 1H), 7.69 (d, *J* = 7.5 Hz, 1H), 7.65 (d, *J* = 8.6 Hz, 1H), 3.66 (s, 2H), 2.87 (s, 4H), 2.70 (s, 4H), 2.57 (s, 3H).^{13}C NMR (126 MHz, $CDCl_3$) δ 163.21, 153.83, 152.19, 147.27, 146.10, 137.63, 136.80, 134.84, 132.07, 131.21, 130.98, 129.46, 128.83 (q, *J* = 30.8 Hz), 127.81, 127.64, 127.22, 124.31, 123.51 (q, *J* = 274.3 Hz), 123.38, 119.60, 118.01 (d, *J* = 5.8 Hz), 114.51, 91.68, 88.49, 57.05, 53.91, 50.37, 43.97.^{19}F NMR (471 MHz, $CDCl_3$) δ -59.23. HRMS $[M]^+$ Calculated for $C_{30}H_{26}F_3N_5O$ 529.2089, found 529.2088.

*4.2.11. The Preparation of 2-(isoquinolin-4-ylethynyl)-N-(4-((4-methylpiperazin-1-yl) methyl)-3-(trifluoromethyl) phenyl) isonicotinamide (**2j**).*

The procedures applied to the synthesis of **1** were used with 2-bromoisonicotinic acid **5-2j** (51 mg, 0.25 mmol), 4-((4-methylpiperazin-1-yl) methyl)-3-(trifluoromethyl) aniline (82 mg, 0.30 mmol) and 4-((trimethylsilyl)ethynyl) isoquinoline **7-1** (112 mg, 0.50 mmol) to obtain **2j** as a brown solid (46 mg, yield: 35%): mp 116~118 ℃. ^{1}H NMR (400 MHz, $CDCl_3$) δ 9.87 (s, 1H), 9.17 (s, 1H), 8.76 (d, *J* = 5.1 Hz, 1H), 8.72 (s, 1H), 8.27 (d, *J* = 8.3 Hz, 1H), 8.20 (s, 1H), 8.06 (s, 1H), 8.02 (d, *J* = 8.3 Hz, 1H), 7.97 (d, *J* = 8.2 Hz, 1H), 7.86 (dd, *J* = 5.1, 1.3 Hz, 1H), 7.76 (t, *J* = 7.4 Hz, 1H), 7.69 – 7.61 (m, 2H), 3.63 (s, 2H), 2.71 (s, 4H), 2.62 (s, 4H), 2.45 (s, 3H).^{13}C NMR (126 MHz, $CDCl_3$) δ 163.19, 152.28, 150.45, 146.37, 143.17, 141.80, 136.47, 134.97, 132.69, 131.27, 130.94, 127.85, 127.56, 127.17, 123.49 (q, *J* = 274.1 Hz), 123.36, 120.57, 117.91 (d, *J* = 6.0 Hz), 114.32, 94.60, 92.56 – 91.55 (m), 85.06, 54.12, 51.02, 44.42.^{19}F NMR (471 MHz, $CDCl_3$) δ -59.29. HRMS $[M]^+$ Calculated for $C_{30}H_{26}F_3N_5O$ 529.2089, found 529.2093.

*4.2.12. The Preparation of 2-(isoquinolin-4-ylethynyl)-N-(4-((4-methylpiperazin-1-yl) methyl)-3-(trifluoromethyl) phenyl) pyrimidine-4-carboxamide (**2k**).*

The procedures applied to the synthesis of **1** were used with 2-chloropyrimidine-4-carboxylic acid **5-2k** (51 mg, 0.25 mmol), 4-((4-methylpiperazin-1-yl) methyl)-3-(trifluoromethyl) aniline (82 mg, 0.30 mmol) and 4-((trimethylsilyl) ethynyl) isoquinoline **7-1** (112 mg, 0.50 mmol) to obtain **2k** as a dark brown solid (20 mg, yield: 15%): mp 102~104 ℃. ^{1}H NMR (400 MHz, $CDCl_3$) δ 9.96 (s, 1H), 9.35 (s, 1H), 9.14 (d, *J* = 5.0 Hz, 1H), 8.99 (s, 1H), 8.46 (d, *J* = 8.5 Hz, 1H), 8.21 (d, *J* = 5.0 Hz, 1H), 8.07 (dd, *J* = 18.4, 8.3 Hz, 3H), 7.91 (t, *J* = 7.6 Hz, 1H), 7.76 (t, *J* = 8.0 Hz, 2H), 3.74 (s, 2H), 2.82 (s, 4H), 2.75 (s, 4H), 2.56 (s, 3H). ^{13}C NMR (126 MHz, $CDCl_3$) δ 160.22, 160.03, 156.56, 153.77, 151.96, 148.14, 135.98, 135.76, 133.51, 131.89, 131.72, 128.45, 128.26, 127.75, 124.97, 123.09, 117.88 (d, *J* = 5.9 Hz), 117.26, 113.81, 94.15, 84.66, 57.69, 54.60, 51.33, 44.85.^{19}F NMR (471 MHz, $CDCl_3$) δ -59.43. HRMS $[M]^+$ Calculated for $C_{29}H_{25}F_3N_6O$ 530.2042, found 530.2045.

*4.2.13. The Preparation of 3-((1H-pyrrolo[2,3-c] pyridin-4-yl) ethynyl)-4-methyl-N-(4-((4-methylpiperazin-1-yl) methyl)-3-(trifluoromethyl) phenyl) benzamide (**3a**).*

The procedures applied to the synthesis of **1** were used with 3-iodo-4-methylbenzoic acid **5-1** (66 mg, 0.25 mmol), 4-((4-methylpiperazin-1-yl) methyl)-3-(trifluoromethyl) aniline (82 mg, 0.30 mmol) and 4-((trimethylsilyl)ethynyl)-1H-pyrrolo[2,3-*c*] pyridine **7-3a** (107 mg, 0.50 mmol) to obtain **3a** as a white solid (62 mg, yield: 47%): mp 160~162 ℃. ^{1}H NMR (400 MHz, CD_3OD_SPE) δ 8.72 (s, 1H), 8.28 (s, 1H), 8.17 (s, 2H), 7.97 (d, *J* = 8.3 Hz, 1H), 7.88 (dd, *J* = 8.0, 1.8 Hz, 1H), 7.75 (d, *J* = 8.5 Hz, 1H), 7.69 (d, *J* = 3.0 Hz, 1H), 7.45 (d, *J* = 8.1 Hz, 1H), 6.77 (d, *J* = 3.0 Hz, 1H), 3.72 (s, 2H), 3.09 (s, 4H), 2.73 (s, 3H), 2.70 (s, 4H), 2.65 (s, 3H).^{13}C NMR (126 MHz, MeOD) δ 165.89, 143.58, 139.08, 137.64, 133.50, 132.54, 131.62, 131.25, 130.75, 130.44, 130.14, 129.15, 128.22 (q, *J* = 30.3 Hz), 127.04, 124.91, 123.83 (q, *J* = 273.2 Hz), 123.24, 122.66, 117.40 (d, *J* = 6.0 Hz), 99.96, 91.14, 89.43, 56.51, 53.41, 49.94, 42.41, 19.25.^{19}F NMR (471 MHz, MeOD) δ -60.29. HRMS $[M]^+$ Calculated for $C_{30}H_{28}F_3N_5O$ 531.5832, found 531.5837.

*4.2.14. The Preparation of 4-methyl-3-((1-methyl-1H-pyrrolo[2,3-c] pyridin-4-yl) ethynyl)-N-(4-((4-methylpiperazin-1-yl) methyl)-3-(trifluoromethyl) phenyl) benzamide (**3b**).*

The procedures applied to the synthesis of **1** were used with 3-iodo-4-methylbenzoic acid **5-1** (66 mg, 0.25 mmol), 4-((4-methylpiperazin-1-yl) methyl)-3-(trifluoromethyl) aniline (82 mg, 0.30 mmol) and 1-methyl-4-((trimethylsilyl)ethynyl)-1H-pyrrolo[2,3-*c*] pyridine **7-3b** (114 mg, 0.50 mmol) to obtain **3b** as a white solid (56 mg, yield: 41%): mp 117~119 ℃. ^{1}H NMR (400 MHz, $CDCl_3$) δ 8.84 (s, 1H), 8.68 (s, 1H), 8.46 (s, 1H), 8.09 (s, 1H), 7.97 (d, *J* = 5.7 Hz, 2H), 7.83 (d, *J* = 8.0 Hz, 1H), 7.74 (d, *J* = 8.8 Hz, 1H), 7.37 (d, *J* = 8.1 Hz, 1H), 7.28 (d, *J* = 3.4 Hz, 1H), 6.68 (d, *J* = 2.9 Hz, 1H), 3.91 (s, 3H), 3.66 (s, 2H), 3.12 (s, 4H), 2.63 (s, 3H), 2.59 (s, 4H), 2.39 (s, 3H).^{13}C NMR (126 MHz, $CDCl_3$) δ 165.40, 144.33, 141.49, 137.16, 134.28, 133.51, 133.11, 133.01, 132.16, 132.02, 131.41, 130.39, 130.08, 129.26 (q, *J* = 30.5 Hz), 127.50, 123.53, 123.43, 117.85 (d, *J* = 6.0 Hz), 111.28, 100.47, 92.00, 90.65, 57.75, 54.80, 52.31, 45.38, 21.02.^{19}F NMR (471 MHz, $CDCl_3$) δ -59.33. HRMS $[M]^+$ Calculated for $C_{31}H_{30}F_3N_5O$ 545.2402, found 545.2405.

*4.2.15. The Preparation of 3-((5-(isopropylamino) pyridin-3-yl) ethynyl)-4-methyl-N-(4-((4-methylpiperazin-1-yl) methyl)-3-(trifluoromethyl) phenyl) benzamide (**3c**).*

The procedures applied to the synthesis of **1** were used with 3-iodo-4-methylbenzoic acid **5-1** (66 mg, 0.25 mmol), 4-((4-methylpiperazin-1-yl) methyl)-3-(trifluoromethyl) aniline (82 mg, 0.30 mmol) and N-isopropyl-5-((trimethylsilyl)ethynyl) pyridin-3-amine **7-3c** (116 mg, 0.50 mmol) to obtain **3c** as a brown solid (70 mg, yield: 51%): mp 121~123 ℃. ^{1}H NMR (400 MHz, CD_3OD_SPE) δ 8.18 (d, *J* = 1.9 Hz, 1H), 8.12 (d, *J* = 1.7 Hz, 1H), 7.98 (d, *J* = 6.8 Hz, 1H), 7.89 (dd, *J* = 8.0, 1.8 Hz, 2H), 7.78 (d, *J* = 8.4 Hz, 1H), 7.46 (d, *J* = 8.0 Hz, 1H), 7.12 (s, 1H), 3.74 (s, 2H), 3.66 (dt, *J* = 12.7, 6.3 Hz, 1H), 3.09 (s, 4H), 2.73 (s, 7H), 2.60 (s, 3H), 1.24 (t, *J* = 6.0 Hz, 6H).^{13}C NMR (126 MHz, $CDCl_3$) δ 166.11, 145.21, 143.67, 140.97, 138.18, 136.42, 132.95, 132.70, 132.19, 131.43, 130.75, 130.02 (q, *J* = 30.6 Hz), 128.36, 124.74 (q, *J* = 274.0 Hz), 124.27, 123.82, 121.24, 120.72, 118.86 (d, *J* = 5.9 Hz), 92.41, 90.07, 58.30, 55.16, 51.75, 45.32, 44.74, 23.39, 21.56.^{19}F NMR (471 MHz, $CDCl_3$) δ -59.27. HRMS $[M]^+$ Calculated for $C_{31}H_{34}F_3N_5O$ 549.2715, found 549.2712.

*4.2.16. The Preparation of 3-((5-(diethylamino) pyridin-3-yl) ethynyl)-4-methyl-N-(4-((4-methylpiperazin-1-yl) methyl)-3-(trifluoromethyl) phenyl) benzamide (**3d**).*

The procedures applied to the synthesis of **1** were used with 3-iodo-4-methylbenzoic acid **5-1** (66 mg, 0.25 mmol), 4-((4-methylpiperazin-1-yl) methyl)-3-(trifluoromethyl) aniline (82 mg, 0.30 mmol) and N, N-diethyl-5-((trimethylsilyl)ethynyl) pyridin-3-amine **7-3d** (123 mg, 0.50 mmol) to obtain **3d** as a brown solid (66 mg, yield: 47%): mp 108~110 ℃. ^{1}H NMR (400 MHz, $CDCl_3$) δ 9.05 (s, 1H), 8.08 (s, 1H), 8.04 (s, 1H), 7.99 (d, *J* = 9.1 Hz, 3H), 7.86 (d, *J* = 7.9 Hz, 1H), 7.60 (d, *J* = 8.2 Hz, 1H), 7.35 (d, *J* = 8.1 Hz, 1H), 7.03 (s, 1H), 3.69 (s, 2H), 3.37 (q, *J* = 7.1 Hz, 4H), 3.04 (d, *J* = 40.2 Hz, 4H), 2.79 (s, 4H), 2.65 (s, 3H), 2.56 (s, 3H), 1.18 (t, *J* = 7.1 Hz, 6H). ^{13}C NMR (126 MHz, $CDCl_3$) δ 164.97, 144.01, 142.54, 138.04, 137.26, 133.13, 131.46, 131.17, 131.05, 130.35, 129.53, 128.91 (q, *J* = 30.7 Hz), 127.17, 123.52 (q, *J* = 274.2 Hz), 123.12, 122.67, 119.46, 119.39, 117.82 (d, *J* = 5.9 Hz), 91.46, 88.62, 57.01, 53.67, 49.68, 43.64, 43.55, 20.38, 11.83. ^{19}F NMR (471 MHz, $CDCl_3$) δ -59.23. HRMS $[M]^+$ Calculated for $C_{32}H_{36}F_3N_5O$ 563.2872, found 563.2877.

*4.2.17. The Preparation of 4-methyl-N-(4-((4-methylpiperazin-1-yl) methyl)-3-(trifluoromethyl) phenyl)-3-((5-(pyrrolidin-1-yl) pyridin-3-yl) ethynyl) benzamide (**3e**).*

The procedures applied to the synthesis of **1** were used with 3-iodo-4-methylbenzoic acid **5-1** (66 mg, 0.25 mmol), 4-((4-methylpiperazin-1-yl) methyl)-3-(trifluoromethyl) aniline (82 mg, 0.30 mmol) and 3-(pyrrolidin-1-yl)-5-((trimethylsilyl)ethynyl) pyridine **7-3e** (122 mg, 0.50 mmol) to obtain **3e** as a brown solid (60 mg, yield: 43%): mp 137~139 ℃. ^{1}H NMR (400 MHz, $CDCl_3$) δ 9.10 (s, 1H), 8.07 (d, *J* = 1.8 Hz, 1H), 8.06 (d, *J* = 1.4 Hz, 1H), 8.01 (d, *J* = 1.9 Hz, 1H), 7.98 (d, *J* = 8.4 Hz, 1H), 7.89 – 7.84 (m, 2H), 7.59 (d, *J* = 8.5 Hz, 1H), 7.33 (d, *J* = 8.1 Hz, 1H), 6.90 (d, *J* = 2.6 Hz, 1H), 3.69 (s, 2H), 3.29 (t, *J* = 6.5 Hz, 4H), 3.03 (s, 4H), 2.81 (d, *J* = 4.3 Hz, 4H), 2.68 (s, 3H), 2.55 (s, 3H), 2.06 – 2.02 (m, 4H). ^{13}C NMR (126 MHz, $CDCl_3$) δ 166.28, 145.08, 143.75, 139.45, 138.44, 134.26, 132.72, 132.62, 132.14, 131.55, 130.66, 129.96 (q, *J* = 30.6 Hz), 128.46, 124.76 (q, *J* = 274.4 Hz), 124.37, 123.78, 120.50, 118.98 (d, *J* = 6.0 Hz), 92.65, 89.88, 58.24, 55.05, 51.40, 47.99, 45.09, 26.06, 21.56. ^{19}F NMR (471 MHz, $CDCl_3$) δ -59.20. HRMS $[M]^+$ Calculated for $C_{32}H_{34}F_3N_5O$ 561.2715, found 561.2713.

*4.2.18. The Preparation of 4-methyl-N-(4-((4-methylpiperazin-1-yl) methyl)-3-(trifluoromethyl) phenyl)-3-((5-morpholinopyridin-3-yl) ethynyl) benzamide (**3f**).*

The procedures applied to the synthesis of **1** were used with 3-iodo-4-methylbenzoic acid **5-1** (66 mg, 0.25 mmol), 4-((4-methylpiperazin-1-yl) methyl)-3-(trifluoromethyl) aniline (82 mg, 0.30 mmol) and 4-(5-((trimethylsilyl)ethynyl) pyridin-3-yl) morpholine **7-3f** (130 mg, 0.50 mmol) to obtain **3f** as a light yellow solid (79 mg, yield: 55%): mp 128~130 ℃. ^{1}H NMR (400 MHz, DMSO) δ 10.66 (s, 1H), 8.37 (d, *J* = 2.8 Hz, 1H), 8.25 (d, *J* = 1.8 Hz, 1H), 8.22 (d, *J* = 1.4 Hz, 1H), 8.21 (d, *J* = 1.5 Hz, 1H), 8.13 (d, *J* = 8.5 Hz, 1H), 7.99 – 7.95 (m, 1H), 7.71 (d, *J* = 8.5 Hz, 1H), 7.52 (d, *J* = 8.2 Hz, 2H), 3.79 – 3.73 (m, 4H), 3.63 (s, 2H), 3.39 (s, 4H), 3.26 – 3.22 (m, 4H), 2.89 (s, 4H), 2.56 (s, 3H), 2.54 (s, 3H). ^{13}C NMR (126 MHz, $CDCl_3$) δ 166.12, 147.02, 145.15, 143.48, 138.41, 137.98, 132.70, 132.50, 132.17, 131.75, 130.69, 129.94 (q, *J* = 30.5 Hz), 128.55, 124.75 (q, *J* = 274.1 Hz), 124.65, 124.39, 123.57, 120.73, 118.99 (d, *J* = 5.5 Hz), 91.88, 90.66, 67.20, 58.19, 54.96, 51.17, 48.84, 44.91, 21.57. ^{19}F NMR (471 MHz, $CDCl_3$) δ -59.15. HRMS $[M]^+$ Calculated

for $C_{32}H_{34}F_3N_5O_2$ 577.2665, found 577.2661.

*4.2.19. The Preparation of 4-methyl-N-(4-((4-methylpiperazin-1-yl) methyl)-3-(trifluoromethyl) phenyl)-3-((5-(4-methylpiperazin-1-yl) pyridin-3-yl) ethynyl) benzamide (**3g**).*

The procedures applied to the synthesis of **1** were used with 3-iodo-4-methylbenzoic acid **5-1** (66 mg, 0.25 mmol), 4-((4-methylpiperazin-1-yl) methyl)-3-(trifluoromethyl) aniline (82 mg, 0.30 mmol) and 1-methyl-4-(5-((trimethylsilyl) ethynyl) pyridin-3-yl) piperazine **7-3g** (137 mg, 0.50 mmol) to obtain **3g** as a dark brown solid (90 mg, yield: 61%): mp 109~111 ℃. ^{1}H NMR (400 MHz, CD_3OD_SPE) δ 8.25 (d, *J* = 2.8 Hz, 1H), 8.15 (dd, *J* = 5.8, 1.8 Hz, 2H), 8.10 (d, *J* = 1.9 Hz, 1H), 7.96 (dd, *J* = 8.4, 2.0 Hz, 1H), 7.87 (dd, *J* = 8.0, 1.9 Hz, 1H), 7.74 (d, *J* = 8.5 Hz, 1H), 7.51 (dd, *J* = 2.7, 1.6 Hz, 1H), 7.43 (d, *J* = 8.2 Hz, 1H), 3.71 (s, 2H), 3.44 – 3.33 (m, 4H), 3.06 (s, 4H), 2.84 – 2.76 (m, 4H), 2.71 (s, 6H), 2.57 (s, 3H), 2.49 (s, 3H).^{13}C NMR (126 MHz, MeOD) δ 166.89, 147.16, 145.02, 142.04, 138.84, 137.36, 132.83, 132.50, 131.95, 131.67, 130.38, 129.40 (q, *J* = 30.2 Hz), 128.48, 125.14, 125.03 (q, *J* = 273.4 Hz), 124.39, 123.27, 121.08, 118.54 (d, *J* = 6.0 Hz), 91.13, 90.42, 57.74, 54.61, 51.20, 47.40, 44.92, 43.66, 20.30.^{19}F NMR (471 MHz, MeOD) δ -60.24. HRMS $[M]^+$ Calculated for $C_{33}H_{37}F_3N_6O$ 590.2981, found 590.2983.

*4.2.20. The Preparation of 3-((5-methoxypyridin-3-yl) ethynyl)-4-methyl-N-(4-((4-methylpiperazin-1-yl) methyl)-3-(trifluoromethyl) phenyl) benzamide (**3h**).*

The procedures applied to the synthesis of **1** were used with 3-iodo-4-methylbenzoic acid **5-1** (66 mg, 0.25 mmol), 4-((4-methylpiperazin-1-yl) methyl)-3-(trifluoromethyl) aniline (82 mg, 0.30 mmol) and 3-methoxy-5-((trimethylsilyl)ethynyl) pyridine **7-3h** (102 mg, 0.50 mmol) to obtain **3h** as a white solid (51 mg, yield: 39%): mp 106~108 ℃. ^{1}H NMR (400 MHz, $CDCl_3$) δ 8.96 (s, 1H), 8.35 (d, *J* = 1.5 Hz, 1H), 8.25 (d, *J* = 2.8 Hz, 1H), 8.07 (d, *J* = 1.6 Hz, 1H), 7.97 (d, *J* = 10.2 Hz, 2H), 7.86 (dd, *J* = 8.0, 1.7 Hz, 1H), 7.62 (d, *J* = 8.2 Hz, 1H), 7.33 (d, *J* = 8.1 Hz, 1H), 7.30 (dd, *J* = 2.7, 1.6 Hz, 1H), 3.87 (s, 3H), 3.66 (s, 2H), 2.91 (s, 4H), 2.73 (s, 4H), 2.59 (s, 3H), 2.55 (s, 3H).^{13}C NMR (126 MHz, $CDCl_3$) δ 166.17, 155.84, 145.16, 144.93, 138.41, 138.10, 132.63, 132.48, 132.06, 131.82, 130.64, 129.82 (q, *J* = 30.5 Hz), 128.68, 124.76 (q, *J* = 274.3 Hz), 124.51, 123.39, 123.03, 121.12, 119.05 (d, *J* = 5.6 Hz), 91.27, 91.07, 58.13, 56.38, 54.93, 51.15, 44.88, 21.51.^{19}F NMR (471 MHz, $CDCl_3$) δ -59.12. HRMS $[M]^+$ Calculated for $C_{29}H_{29}F_3N_4O_2$ 522.2243, found 522.2239.

*4.2.21. The Preparation of 4-chloro-N-(4-((4-methylpiperazin-1-yl) methyl)-3-(trifluoromethyl) phenyl)-3-((5-morpholinopyridin-3-yl) ethynyl) benzamide (**4**).*

The procedures applied to the synthesis of **1** were used with 4-chloro-3-iodobenzoic acid **5-2c** (70 mg, 0.25 mmol), 4-((4-methylpiperazin-1-yl) methyl)-3-(trifluoromethyl) aniline (82 mg, 0.30 mmol) and 4-(5-((trimethylsilyl)ethynyl) pyridin-3-yl) morpholine **7-3f** (130 mg, 0.50 mmol) to obtain **4** as a white solid (87 mg, yield: 58%): mp 132~134 ℃. ^{1}H NMR (400 MHz, $CDCl_3$) δ 9.34 (s, 1H), 8.28 (s, 1H), 8.20 (d, *J* = 2.7 Hz, 1H), 8.16 (d, *J* = 1.8 Hz, 1H), 7.99 (d, *J* = 9.5 Hz, 2H), 7.92 (dd, *J* = 8.4, 1.8 Hz, 1H), 7.63 (d, *J* = 8.3 Hz, 1H), 7.52 (d, *J* = 8.4 Hz, 1H), 7.29 (s, 1H), 3.90 – 3.83 (m, 4H), 3.66 (s, 2H), 3.23 – 3.16 (m, 4H), 2.85 (s, 4H), 2.70 (s, 4H), 2.56 (s, 3H).^{13}C NMR (126 MHz, $CDCl_3$) δ 164.08, 145.81, 142.34, 139.04, 137.10, 136.90, 132.50, 131.89, 131.83, 130.98, 129.25, 128.79 (q, 30.7 Hz), 128.36, 123.58, 123.52 (q, *J* = 274.2 Hz), 123.25, 122.46, 119.02, 117.83 (d, *J* = 6.0 Hz), 91.99, 87.37, 65.99, 57.06, 50.42, 47.58, 44.07.^{19}F NMR

(471 MHz, $CDCl_3$) δ -59.16. HRMS $[M]^+$ Calculated for $C_{31}H_{31}ClF_3N_5O_2$ 597.2118, found 597.2119.

4.3 ELISA Kinase Assay

The effects of indicated compound on the activities of receptor tyrosine kinases were determined using enzyme-linked immunosorbent assays (ELISAs) with purified recombinant proteins. Briefly, 20 μg/mL poly (Glu,Tyr) 4:1 (Sigma, St. Louis, MO, USA) was pre-coated in 96-well plates as a substrate. A 50-μL aliquot of 10 μmol/L ATP solution diluted in kinase reaction buffer (50 mmol/L HEPES [pH 7.4], 50 mmol/L $MgCl_2$, 0.5 mmol/L $MnCl_2$, 0.2 mmol/L Na_3VO_4, and 1 mmol/L DTT) was added to each well; 1 μL of various concentrations of indicated compound diluted in 1% DMSO (v/v) (Sigma) were then added to each reaction well. DMSO (1%, v/v) was used as the negative control. The kinase reaction was initiated by the addition of purified or commercial tyrosine kinase proteins diluted in 49 μL of kinase reaction buffer. After incubation for 60 min at 37 °C, the plate was washed three times with phosphate-buffered saline (PBS) containing 0.1% Tween 20 (T-PBS). Anti-phosphotyrosine (PY99) antibody (100 μL; 1:500, diluted in 5 mg/mL BSA T-PBS) was then added. After a 30-min incubation at 37 °C, the plate was washed three times, and 100 μL horseradish peroxidase-conjugated goat anti-mouse IgG (1:2000, diluted in 5 mg/mL BSA T-PBS) was added. The plate was then incubated at 37 °C for 30 min and washed 3 times. A 100-μL aliquot of a solution containing 0.03% H_2O_2 and 2 mg/ml o-phenylenediamine in 0.1 mol/L citrate buffer (pH 5.5) was added. The reaction was terminated by the addition of 50 μL of 2 mol/L H_2SO_4 as the color changed, and the plate was analyzed using a multi-well spectrophotometer (SpectraMAX 190, Molecular Devices, and Sunnyvale, CA, USA) at 490 nm. The inhibition rate (%) was calculated using the following equation: [1 − (A490/A490 control)] × 100%. The IC_{50} values were calculated from the inhibition curves in two separate experiments.

4.4 Western Blot Analysis

KG1 and SNU16 cells were treated with indicated concentrations of compounds for 2 h at 37°C followed by lysed in 1×SDS sample buffer. Cell lysates were subsequently resolved by SDS–PAGE and transferred to nitrocellulose membranes. The membranes were probed with the appropriate primary antibodies [phospho-FGFR1, phospho-FGFR2, FGFR, phospho-PLCγ, PLCγ, phospho-ERK1/2, ERK1/2 (all from Cell Signaling Technology, Beverly, MA, USA), GAPDH (Epitomics, Burlingame, CA, USA)], and then with horseradish peroxidase-conjugated anti-rabbit or antimouse IgG. The immunoreactive proteins were detected using an enhanced chemiluminescence detection reagent (Thermo Fisher Scientific, Rockford, IL, USA) and images were captured with ImageQuant LAS 4000 (GE Healthcare, Little Chalfont, Buckinghamshire, UK.).

4.5 Cell Proliferation Assay

Cells were seeded in 96-well tissue culture plates. On the next day, cells were exposed to various concentrations of compounds and further cultured for 72 h. Finally, cell proliferation was determined using sulforhodamine B (SRB) assay or Cell Counting Kit(CCK-8) assay. IC_{50} values were calculated by concentration–response curve fitting using a Soft Max pro-based four-parameter method.

4.6 In vivo Antitumor Activity Assay

Male nude mice (4–6 weeks old) were housed and maintained under specific-pathogen free conditions. Animal procedures were performed according to institutional ethical guidelines of animal care. The cells at a density of 5×10^6 in 200 μL were injected s.c. into the right flank of nude mice and then allowed to grow to 700–800 mm^3, defined as a well-developed tumor. After that, the well-developed tumors were cut into 1 mm^3 fragments and transplanted s.c. into the right flank of nude mice using a trocar. When the mean tumor volume reached 120–150 mm^3, the mice were randomly assigned into vehicle and treatment groups (n = 6 in treated group, n = 12 in vehicle group). Vehicle groups were given vehicle alone, and treatment groups received the compound as indicated doses orally once daily for 10 days in NCI-H1581 model and 18 days in SNU16 model. The sizes of the tumors were measured twice per week using microcaliper. The tumor volume (V) was calculated as follows: V = [length (mm) ×width^2 (mm^2)]/2. The individual relative tumor volume (RTV) was calculated as follows: RTV = V_t/V_0, where V_t is the volume on each day, and V_0 represents the volume at the beginning of the treatment. RTV was shown on indicated days as mean ± SD indicated for groups of mice. Percent (%) inhibition values （TGI） were measured on the final day of study for drug-treated compared with vehicle-treated mice and were calculated as $100\% \times (1 - ((\text{treated}^{\text{final day}} - \text{treated}^{\text{day 0}})/(\text{control}^{\text{final day}} - \text{control}^{\text{day 0}})))$.

5. Statistical Analysis

Data of *in vitro and in vivo* efficacy are presented as the mean ± SD, and significance was determined by Student's *t*-test. Differences were considered statistically significant at ***P<0.001, **P<0.01.

Acknowledgments

We are grateful for financial support from the National Natural Science Foundation of China (Grant No. 81225022, 81473243, 81321092); The National Science & Technology Major Project "Key New Drug Creation and Manufacturing Program" of China (Grant No. 2012ZX09301001-007). SA-SIBS Scholarship Program is also gratefully acknowledged.

References

[1] N. Turner, R. Grose, Fibroblast growth factor signaling: from development to cancer. *Nat. Rev. Cancer* **2010,** *10*, 116-129.

[2] M. V. Dieci, M. Arnedos, F. Andre, J. C. Soria, Fibroblast Growth Factor Receptor Inhibitors as a Cancer Treatment: From a Biologic Rationale to Medical Perspectives. *Cancer Discovery* **2013,** *3*, 264-279.

[3] M. Touat, E. Ileana, S. Postel-Vinay, F. Andre, J. C. Soria, Targeting FGFR Signaling in Cancer. *Clin. Cancer Res.* **2015,** *21*, 2684-2694.

[4] J. Weiss, M. L. Sos, D. Seidel, M. Peifer, T. Zander, J. M. Heuckmann, R. T. Ullrich, R. Menon, S. Maier, A. Soltermann, H. Moch, P. Wagener, F. Fischer, S. Heynck, M. Koker, J. Schottle, F. Leenders, F. Gabler, I. Dabow, S. Querings, L. C. Heukamp, H. Balke-Want, S. Ansen, D. Rauh, I. Baessmann, J. Altmuller, Z. Wainer, M. Conron, G. Wright, P. Russell, B. Solomon, E. Brambilla, C. Brambilla, P. Lorimier, S. Sollberg, O. T. Brustugun, W. Engel-Riedel, C. Ludwig, I. Petersen, J. Sanger, J. Clement, H. Groen, W. Timens, H. Sietsma, E. Thunnissen, E. Smit, D. Heideman, F. Cappuzzo, C. Ligorio, S. Damiani, M. Hallek, R. Beroukhim, W. Pao, B. Klebl, M. Baumann, R. Buettner, K. Ernestus, E. Stoelben, J. Wolf, P. Nurnberg, S. Perner, R. K. Thomas, Frequent and focal FGFR1 amplification associates with therapeutically tractable FGFR1 dependency in

squamous cell lung cancer. *Sci. Transl. Med.* **2010,** *2*, 62ra93.

[5] K. Matsumoto, T. Arao, T. Hamaguchi, Y. Shimada, K. Kato, I. Oda, H. Taniguchi, F. Koizumi, K. Yanagihara, H. Sasaki, K. Nishio, Y. Yamada, FGFR2 gene amplification and clinicopathological features in gastric cancer. *Br. J. Cancer* **2012,** *106*, 727-732.

[6] N. Cancer Genome Atlas Research, Comprehensive molecular characterization of urothelial bladder carcinoma. *Nature* **2014,** *507*, 315-322.

[7] N. Turner, A. Pearson, R. Sharpe, M. Lambros, F. Geyer, M. A. Lopez-Garcia, R. Natrajan, C. Marchio, E. Iorns, A. Mackay, C. Gillett, A. Grigoriadis, A. Tutt, J. S. Reis, A. Ashworth, FGFR1 Amplification Drives Endocrine Therapy Resistance and Is a Therapeutic Target in Breast Cancer. *Cancer Res.* **2010,** *70*, 2085-2094.

[8] S. A. Kono, M. E. Marshall, K. E. Ware, L. E. Heasley, The fibroblast growth factor receptor signaling pathway as a mediator of intrinsic resistance to EGFR-specific tyrosine kinase inhibitors in non-small cell lung cancer. *Drug Resist. Updat.* **2009,** *12*, 95-102.

[9] C. Lieu, J. Heymach, M. Overman, H. Tran, S. Kopetz, Beyond VEGF: inhibition of the fibroblast growth factor pathway and antiangiogenesis. *Clin. Cancer Res.* **2011,** *17*, 6130-6139.

[10] J. H. Tchaicha, E. A. Akbay, A. Altabef, O. R. Mikse, E. Kikuchi, K. Rhee, R. G. Liao, R. T. Bronson, L. M. Sholl, M. Meyerson, P. S. Hammerman, K. K. Wong, Kinase domain activation of FGFR2 yields high-grade lung adenocarcinoma sensitive to a Pan-FGFR inhibitor in a mouse model of NSCLC. *Cancer Res.* **2014,** *74*, 4676-4684.

[11] R. G. Liao, J. Jung, J. Tchaicha, M. D. Wilkerson, A. Sivachenko, E. M. Beauchamp, Q. Liu, T. J. Pugh, C. S. Pedamallu, D. N. Hayes, N. S. Gray, G. Getz, K. K. Wong, R. I. Haddad, M. Meyerson, P. S. Hammerman, Inhibitor-sensitive FGFR2 and FGFR3 mutations in lung squamous cell carcinoma. *Cancer Res.* **2013,** *73*, 5195-5205.

[12] P. Ghatalia, C. J. Morgan, T. K. Choueiri, P. Rocha, G. Naik, G. Sonpavde, Pancreatitis with vascular endothelial growth factor receptor tyrosine kinase inhibitors. *Crit. Rev. Oncol. Hematol.* **2015,** *94*, 136-145.

[13] D. R. Talbert, K. R. Doherty, P. B. Trusk, D. M. Moran, S. A. Shell, S. Bacus, A multi-parameter in vitro screen in human stem cell-derived cardiomyocytes identifies ponatinib-induced structural and functional cardiac toxicity. *Toxicol Sci* **2015,** *143*, 147-155.

[14] P. Valent, E. Hadzijusufovic, G. H. Schernthaner, D. Wolf, D. Rea, P. le Coutre, Vascular safety issues in CML patients treated with BCR/ABL1 kinase inhibitors. *Blood* **2015,** *125*, 901-906.

[15] J. Drevs, P. Siegert, M. Medinger, K. Mross, R. Strecker, U. Zirrgiebel, J. Harder, H. Blum, J. Robertson, J. M. Jurgensmeier, T. A. Puchalski, H. Young, O. Saunders, C. Unger, Phase I clinical study of AZD2171, an oral vascular endothelial growth factor signaling inhibitor, in patients with advanced solid tumors. *J. Clin. Oncol.* **2007,** *25*, 3045-3054.

[16] D. Sarker, R. Molife, T. R. Evans, M. Hardie, C. Marriott, P. Butzberger-Zimmerli, R. Morrison, J. A. Fox, C. Heise, S. Louie, N. Aziz, F. Garzon, G. Michelson, I. R. Judson, D. Jadayel, E. Braendle, J. S. de Bono, A phase I pharmacokinetic and pharmacodynamic study of TKI258, an oral, multitargeted receptor tyrosine kinase inhibitor in patients with advanced solid tumors. *Clin. Cancer Res.* **2008,** *14*, 2075-2081.

[17] R. A. Norman, A.-K. Schott, D. M. Andrews, J. Breed, K. M. Foote, A. P. Garner, D. Ogg, J. P. Orme, J. H. Pink, K. Roberts, D. A. Rudge, A. P. Thomas, A. G. Leach, Protein–Ligand Crystal Structures Can Guide the Design of Selective Inhibitors of the FGFR Tyrosine Kinase. *J. Med. Chem.* **2012,** *55*, 5003-5012.

[18] G. S. Zhao, W. Y. Li, D. H. Chen, J. R. Henry, H. Y. Li, Z. G. Chen, M. Zia-Ebrahimi, L. Bloem, Y. Zhai, K. Huss, S. B. Peng, D. J. McCann, A novel, selective inhibitor of fibroblast growth factor receptors that shows a potent broad spectrum of antitumor activity in several tumor xenograft models. *Mol. Cancer Ther.* **2011,** *10*, 2200-2210.

[19] P. R. Gavine, L. Mooney, E. Kilgour, A. P. Thomas, K. Al-Kadhimi, S. Beck, C. Rooney, T. Coleman, D. Baker, M. J. Mellor, A. N. Brooks, T. Klinowska, AZD4547: an orally bioavailable, potent, and selective inhibitor of the fibroblast growth factor receptor tyrosine kinase family. *Cancer Res* **2012,** *72*, 2045-2056.

[20] V. Guagnano, A. Kauffmann, S. Wohrle, C. Stamm, M. Ito, L. Barys, A. Pornon, Y. Yao, F. Li, Y. Zhang, Z. Chen, C. J. Wilson, V. Bordas, M. Le Douget, L. A. Gaither, J. Borawski, J. E. Monahan, K. Venkatesan, T. Brummendorf, D. M. Thomas, C. Garcia-Echeverria, F. Hofmann, W. R. Sellers, D. Graus-Porta, FGFR genetic alterations predict for sensitivity to NVP-BGJ398, a selective pan-FGFR inhibitor. *Cancer Discov.* **2012,** *2*, 1118-1133.

[21] Y. Nakanishi, N. Akiyama, T. Tsukaguchi, T. Fujii, K. Sakata, H. Sase, T. Isobe, K. Morikami, H. Shindoh, T. Mio, H. Ebiike, N. Taka, Y. Aoki, N. Ishii, The Fibroblast Growth Factor Receptor Genetic Status as a Potential Predictor of the Sensitivity to CH5183284/Debio 1347, a Novel Selective FGFR Inhibitor. *Mol. Cancer Ther.* **2014,** *13*, 2547-2558.

[22] J. Tabernero, R. Bahleda, R. Dienstmann, J. R. Infante, A. Mita, A. Italiano, E. Calvo, V. Moreno, B. Adamo, A. Gazzah, B. Zhong, S. J. Platero, J. W. Smit, K. Stuyckens, M. Chatterjee-Kishore, J. Rodon, V. Peddareddigari, F. R. Luo, J. C. Soria, Phase I Dose-Escalation Study of JNJ-42756493, an Oral Pan-Fibroblast Growth Factor Receptor Inhibitor, in Patients with Advanced Solid Tumors. *J. Clin. Oncol.* **2015,** *33*, 3401-3408.

[23] J. M. Gozgit, M. J. Wong, L. Moran, S. Wardwell, Q. K. Mohemmad, N. I. Narasimhan, W. C. Shakespeare, F. Wang, T. Clackson, V. M. Rivera, Ponatinib (AP24534), a multitargeted pan-FGFR inhibitor with activity in multiple FGFR-amplified or mutated cancer models. *Mol. Cancer Ther.* **2012,** *11*, 690-699.

[24] W. S. Huang, C. A. Metcalf, R. Sundaramoorthi, Y. Wang, D. Zou, R. M. Thomas, X. Zhu, L. Cai, D. Wen, S. Liu, J. Romero, J. Qi, I. Chen, G. Banda, S. P. Lentini, S. Das, Q. Xu, J. Keats, F. Wang, S. Wardwell, Y. Ning, J. T. Snodgrass, M. I. Broudy, K. Russian, T. Zhou, L. Commodore, N. I. Narasimhan, Q. K. Mohemmad, J. Iuliucci, V. M. Rivera, D. C. Dalgarno, T. K. Sawyer, T. Clackson, W. C. Shakespeare, Discovery of 3-[2-(imidazo [1,2-*b*] pyridazin-3-yl) ethynyl]-4-methyl-N-{4-[(4-methylpiperazin-1-y l)methyl]-3-(trifluoromethyl) phenyl} benzamide (AP24534), a potent, orally active pan-inhibitor of breakpoint cluster region-abelson (BCR-ABL) kinase including the T315I gatekeeper mutant. *J. Med. Chem.* **2010,** *53*, 4701-4719.

[25] X. Liu, A. Kung, B. Malinoski, G. K. Prakash, C. Zhang, Development of Alkyne-Containing Pyrazolopyrimidines to Overcome Drug Resistance of Bcr-Abl Kinase. *J Med Chem* **2015,** *58*, 9228-9237.

[26] X. Ren, X. Pan, Z. Zhang, D. Wang, X. Lu, Y. Li, D. Wen, H. Long, J. Luo, Y. Feng, X. Zhuang, F. Zhang, J. Liu, F. Leng, X. Lang, Y. Bai, M. She, Z. Tu, J. Pan, K. Ding, Identification of GZD824 as an orally bioavailable inhibitor that targets phosphorylated and nonphosphorylated breakpoint cluster Region-Abelson (Bcr-Abl) kinase and overcomes clinically acquired mutation-induced resistance against imatinib. *J. Med. Chem.* **2013,** *56*, 879-894.

[27] Y. Li, M. Shen, Z. Zhang, J. Luo, X. Pan, X. Lu, H. Long, D. Wen, F. Zhang, F. Leng, Y. Li, Z. Tu, X. Ren, K. Ding, Design, Synthesis, and Biological Evaluation of

3-(1H-1,2,3-Triazol-1-yl)benzamide Derivatives as Potent Pan Bcr-Abl Inhibitors Including the Threonine315→Isoleucine315 Mutant. *J. Med. Chem.* **2012,** *55*, 10033-10046.

[28] X. Lu, Z. Zhang, X. Ren, X. Pan, D. Wang, X. Zhuang, J. Luo, R. Yu, K. Ding, Hybrid pyrimidine alkynyls inhibit the clinically resistance related Bcr-AblT315I mutant. *Bioorg. Med. Chem. Lett.* **2015,** *25*, 3458-3463.

[29] M. Thomas, W. S. Huang, D. Wen, X. Zhu, Y. Wang, C. A. Metcalf, S. Liu, I. Chen, J. Romero, D. Zou, R. Sundaramoorthi, F. Li, J. Qi, L. Cai, T. Zhou, L. Commodore, Q. Xu, J. Keats, F. Wang, S. Wardwell, Y. Ning, J. T. Snodgrass, M. I. Broudy, K. Russian, J. Iuliucci, V. M. Rivera, T. K. Sawyer, D. C. Dalgarno, T. Clackson, W. C. Shakespeare, Discovery of 5-(arenethynyl) hetero-monocyclic derivatives as potent inhibitors of BCR-ABL including the T315I gatekeeper mutant. *Bioorg. Med. Chem. Lett.* **2011,** *21*, 3743-3748.

[30] M. Gao, L. Duan, J. Luo, L. Zhang, X. Lu, Y. Zhang, Z. Zhang, Z. Tu, Y. Xu, X. Ren, K. Ding, Discovery and Optimization of 3-(2-(Pyrazolo[1,5-a]pyrimidin-6-yl)ethynyl)benzamides as Novel Selective and Orally Bioavailable Discoidin Domain Receptor 1 (DDR1) Inhibitors. *J. Med. Chem.* **2013,** *56*, 3281-3295.

[31] C.-H. Zhang, M.-W. Zheng, Y.-P. Li, X.-D. Lin, M. Huang, L. Zhong, G.-B. Li, R.-J. Zhang, W.-T. Lin, Y. Jiao, X.-A. Wu, J. Yang, R. Xiang, L.-J. Chen, Y.-L. Zhao, W. Cheng, Y.-Q. Wei, S.-Y. Yang, Design, Synthesis, and Structure–Activity Relationship Studies of 3-(Phenylethynyl)-1H-pyrazolo[3,4-d] pyrimidin-4-amine Derivatives as a New Class of Src Inhibitors with Potent Activities in Models of Triple Negative Breast Cancer. *J. Med. Chem.* **2015,** *58*, 3957-3974.

[32] L. M. Mulligan, RET revisited: expanding the oncogenic portfolio. *Nat. Rev. Cancer* **2014,** *14*, 173-186.

Table, Figure and Scheme Captions

Table 1. FGFR1/KDR enzymatic and FGFR1 translocated KG1 cellular activities of the designed Ponatinib derivatives **1**-**2**.

Table 2. FGFR1/KDR enzymatic and FGFR1 translocated KG1 cellular activities of the designed Ponatinib derivatives **3**-**4**.

Table3. Kinase selectivity profiles and anti-proliferative activity for the related cell lines displayed by **4** and Ponatinib.

Figure 1. Ponatinib analogues with different biological activities and the strategy for discovery of novel selective FGFRs inhibitors.

Figure 2. Compound **4** suppresses FGFR phosphorylation and downstream signaling in KG1 Cells (A) and SNU16 cells (B). Cells were treated with indicated concentrations of **4** for 2 hr and analyzed by using immunoblotting.

Figure 3. Plasma concentration vs time plots after oral administration of 10 mg/kg of compound **4**. Plasma concentration was monitored at 0.5, 1, 2, 3, 5, 7, 9, 12 and 24 h after dosing.

Figure 4. Compound **4** potently inhibits FGFR-dependent tumor growth through effects on tumor cell growth as well as through antiangiogenic mechanisms. Inhibitory activity of **4** on tumor growth in NCI-H1581 (A) and SNU16 (B) xenografts. **4** was administrated to the tumor-bearing mice once a day for 10 or 18 d. Mean relative tumor volume ± SE on the final day is shown (n = 6 per group).

Scheme 1. Synthetic route of designed compounds **1**-**4**.

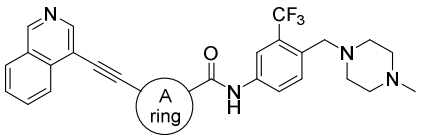

1, 2

Compound	A ring	IC_{50} (nM)		KDR (nM)
		FGFR1	KG1 (Cell)	
1	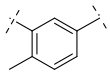	1.2± 0.4	175.4±49.5	79.1±3.0
2a	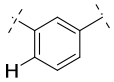	1.1±0.5	67.6 ±11.5	2.5 ± 0.5
2b	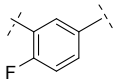	1.3 ±0.5	27.8 ±10.3	5.5 ± 1.6
2c	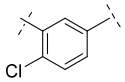	5.2± 0.7	88.2± 21.9	91.4 ±8.1
2d	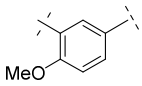	26.5±7.8	> 500	NT[b]
2e	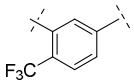	> 100	> 500	NT[b]
2f	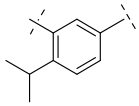	> 100	NT[b]	NT[b]
2g	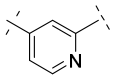	8.1±2.6	> 500	NT[b]
2h	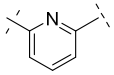	> 100	NT[b]	NT[b]
2i	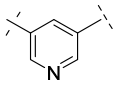	1.6±0.3	>500	2.6±0.2
2j	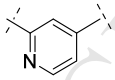	2.2±0.4	427.1 ±21.4	6.5 ± 0.5
2k	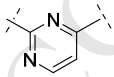	11.2±1.6	> 500	NT[b]

[a]IC_{50} values are given as the mean±SD (nM) from two separate experiments. [b]Not tested.

Table 1. FGFR1/KDR enzymatic and FGFR1 translocated KG1 cellular activities of the designed Ponatinib derivatives **1-2**.[a]

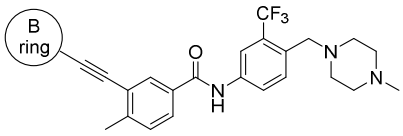

3

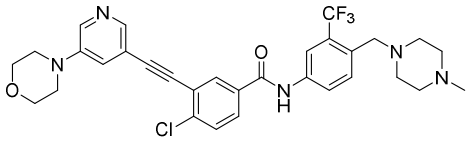

4

Compound	B ring	IC_{50} (nM)		KDR (nM)
		FGFR1	KG1 (Cell)	
3a	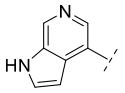	6.7 ± 2.3	489.8±140.8	> 100
3b	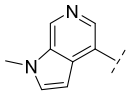	1.1 ± 0.2	10.0 ± 5.9	63.5±2.6
3c	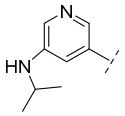	3.6 ± 1.9	84.5 ± 24.3	59.9 ±3.8
3d	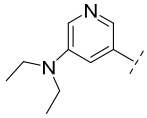	6.5 ± 2.6	58.3 ± 5.8	104.5±4.7
3e	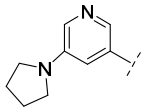	7.6 ± 1.5	119.2± 18.2	108.1±15.6
3f	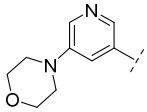	3.0 ± 1.8	24.3 ± 7.6	89.9± 13.4
3g	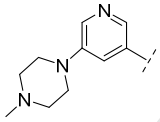	5.7 ± 1.4	21.7 ± 3.7	21.8 ± 4.8
3h	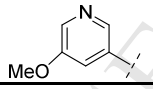	12.8±2.2	125.2±45.9	110.2±27.3
4		0.5 ± 0.0	7.5 ± 3.6	48.7 ± 0.1

[a]IC_{50} values are given as the mean±SD (nM) from two separate experiments. [b]Not tested.

Table 2. FGFR1/KDR enzymatic and FGFR1 translocated KG1 cellular activities of the designed Ponatinib derivatives 3-4.[a]

Kinase	IC_{50} (nM)		Cell lines[b]	IC_{50} (nM)	
	4	Ponatinb		**4**	Ponatinib
FGFR1	0.5±0.0	1.2±0.1	KG1	7.5±3.6	17.2±3.8
			H1581	57.0±2.8	194.2±29.5
FGFR2	0.3±0.1	1.3±0.2	SNU16	26.4±0.9	33.6±2.1
FGFR3	1.0±0.1	9.4±2.3	RT112	514.4±1.2	736.5±55.5
FGFR4	5.5±0.6	7.1±1.1	BaF3/TEL-FGFR4	131.0±8.1	126.8±4.5
KDR	48.7±0.1	3.7±1.5	BaF3/TEL-KDR	489.0±42.2	53.7±11.2
RET	1.3±0.3	0.3±0.1	BaF3/CCDC6-RET	37.2±3.9	39.1±2.6
RETV804M	7.5±1.3	1.9±0.3	BaF3/CCDC6-RET-V804M	33.4±5.4	71.5±2.4
VEGFR1	62.7±6.4	20.9±0.8	-	-	-
EGFR	>100	>1000	-	-	-
PDGFR-α	5.6±0.3	2.6±0.4	-	-	-
PDGFR-β	5.5±0.9	1.2±02	-	-	-
c-Src	10.8±1.5	2.5±0.6	-	-	-
ABL	23.2±1.1	7.7±0.1	-	-	-

[a]IC_{50} values are given as the mean ± SD (nM) or estimated values from two separate experiments. [b]Cell line KG1, H1581, KATOIII, SNU16, RT112 are driven by FGFR1 translocation, FGFR1 amplification, FGFR2 amplification, FGFR2 amplification, FGFR3 amplification, respectively. BaF3/TEL-FGFR4, BaF3/TEL-KDR, BaF3/CCDC6-RET, BaF3/CCDC6-RET-V804M cells were stably expressing constitutively active oncogenic version TEL-FGFR4, TEL-KDR, CCDC6-RET, CCDC6-RET-V804M respectively.

Table 3. Kinase selectivity profiles and selected anti-proliferative activity for the related cell lines displayed by **4** and Ponatinib.[a]

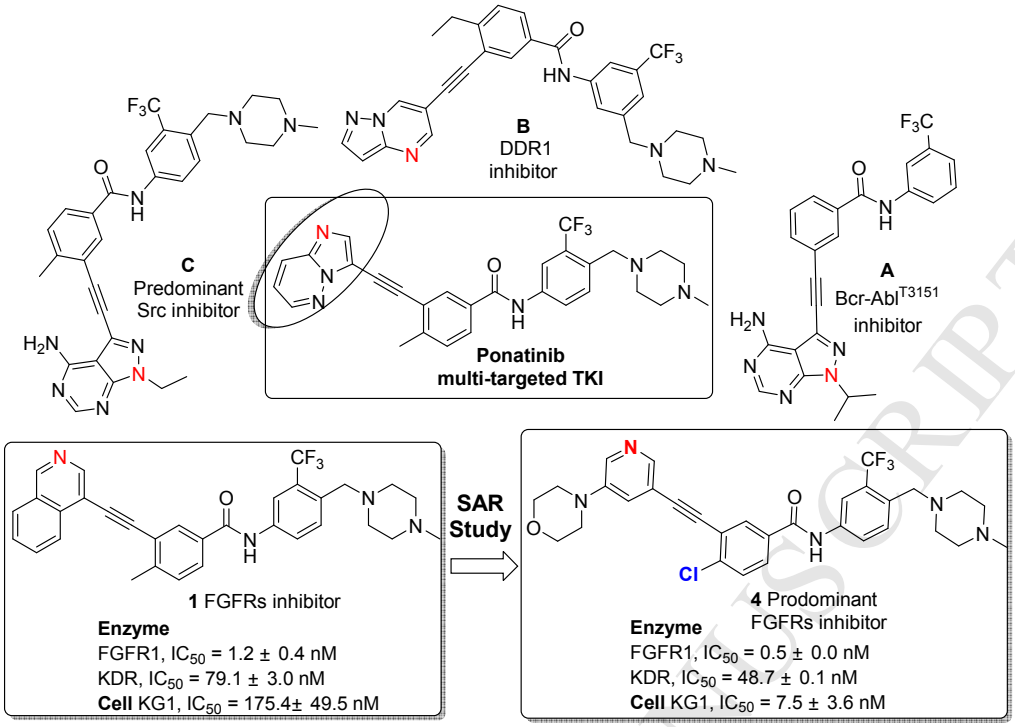

Figure 1. Ponatinib analogues with different biological activities and the strategy for discovery of novel selective FGFRs inhibitors.

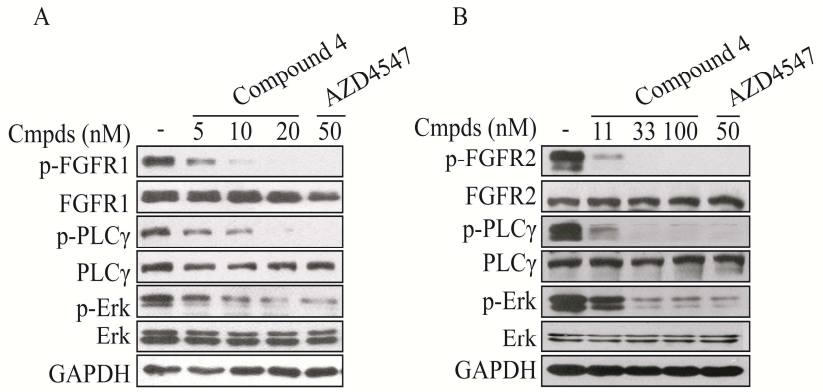

Figure 2. Compound **4** suppresses FGFR phosphorylation and downstream signaling in KG1 Cells (A) and SNU16 cells (B). Cells were treated with indicated concentrations of **4** for 2 hr and analyzed by using immunoblotting.

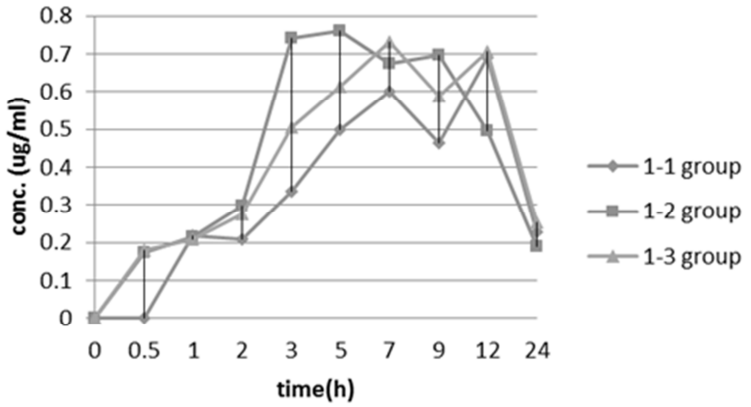

Figure 3. Plasma concentration vs time plots after oral administration of 10 mg/kg of compound **4**. Plasma concentration was monitored at 0.5, 1, 2, 3, 5, 7, 9, 12 and 24 h after dosing.

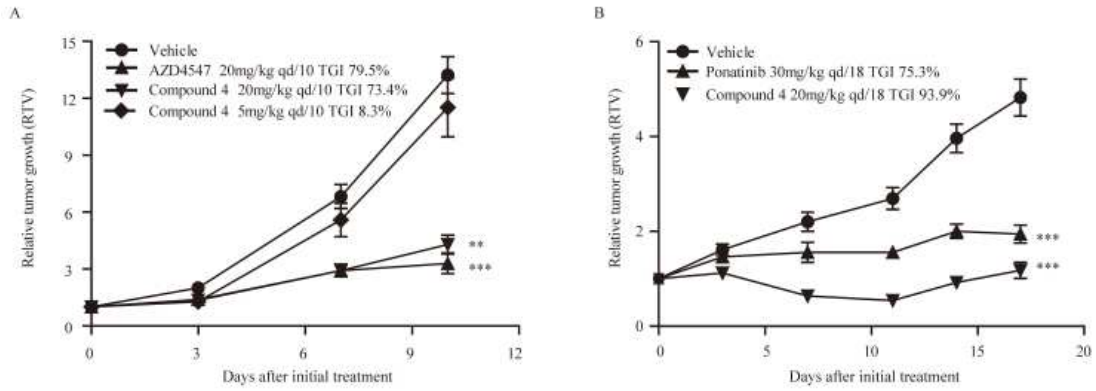

Figure 4. Compound **4** potently inhibits FGFR-dependent tumor growth through effects on tumor cell growth as well as through antiangiogenic mechanisms. Inhibitory activity of **4** on tumor growth in NCI-H1581 (A) and SNU16 (B) xenografts. **4** was administrated to the tumor-bearing mice once a day for 10 or 18 d. Mean relative tumor volume ± SE on the final day is shown (n = 6 per group).

.

Scheme 1. Synthetic route of designed compounds **1-4**[a].

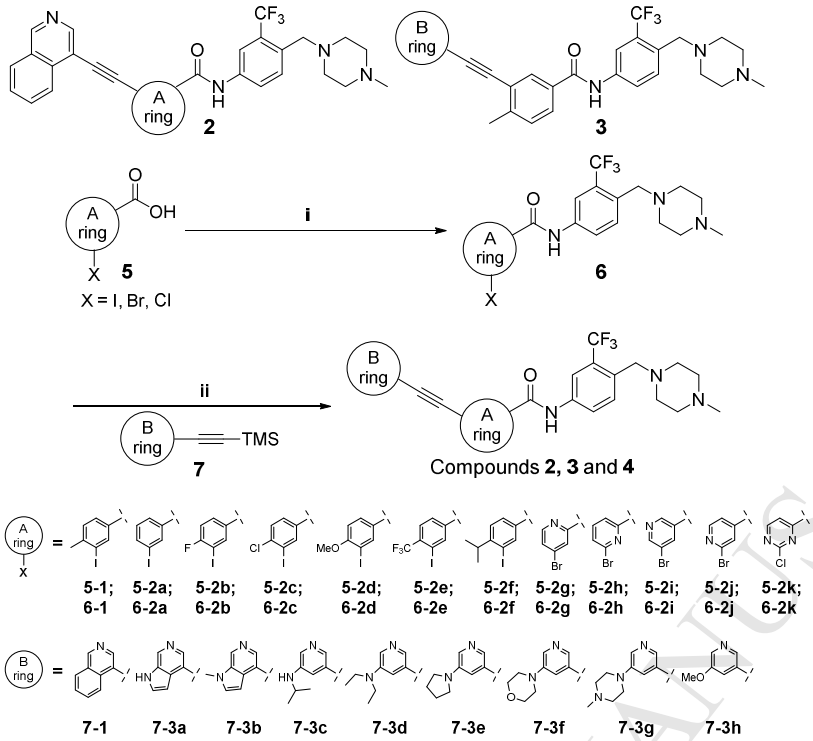

[a]Reagents and conditions: (i) (a) Oxalyl chloride, DMF (cat.), CH_2Cl_2, rt, 3 h; (b) 4-((4-methylpiperazin-1-yl)methyl)-3-(trifluoromethyl)aniline, Et_3N, CH_2Cl_2, rt, 5h; (ii) **7**, $Pd(PPh_3)_4$, CuI, Et_3N, CsF, MeCN, MW: 90 ^oC, 15 min.